Research Paper

A Two-tiered compensatory response to loss of DNA repair modulates aging and stress response pathways

Øyvind Fensgård[1], Henok Kassahun[1], Izabela Bombik[1], Torbjørn Rognes[2], Jessica Margareta Lindvall[2] and Hilde Nilsen[1]

[1] University of Oslo, The Biotechnology Centre, P.O. Box 1125 Blindern, 0317 Oslo, Norway.
[2] University of Oslo, Department of Informatics, P.O. Box 1080 Blindern, NO-0316 Oslo, Norway

Running title: *Compensatory response in DNA repair mutants*
Key words: *DNA repair, Caenorhabditis elegans, aging, gene expression profiling, Base Excision Repair, Nucleotide Excision Repair*
Correspondence: *Hilde Nilsen, PhD, University of Oslo, The Biotechnology Centre, PO Box 1125 Blindern, 0317 Oslo, Norway*
Received: *03/10/10; accepted: 03/27/10; published on line: 03/29/10*
E-mail: *hilde.nilsen@biotek.uio.no*

Abstract: Activation of oxidative stress-responses and downregulation of insulin-like signaling (ILS) is seen in Nucleotide Excision Repair (NER) deficient segmental progeroid mice. Evidence suggests that this is a survival response to persistent transcription-blocking DNA damage, although the relevant lesions have not been identified. Here we show that loss of NTH-1, the only Base Excision Repair (BER) enzyme known to initiate repair of oxidative DNA damage in *C. elegans*, restores normal lifespan of the short-lived NER deficient *xpa-1* mutant. Loss of NTH-1 leads to oxidative stress and global expression profile changes that involve upregulation of genes responding to endogenous stress and downregulation of ILS. A similar, but more extensive, transcriptomic shift is observed in the *xpa-1* mutant whereas loss of both NTH-1 and XPA-1 elicits a different profile with downregulation of Aurora-B and Polo-like kinase 1 signaling networks as well as DNA repair and DNA damage response genes. The restoration of normal lifespan and absence oxidative stress responses in *nth-1;xpa-1* indicate that BER contributes to generate transcription blocking lesions from oxidative DNA damage. Hence, our data strongly suggests that the DNA lesions relevant for aging are repair intermediates resulting from aberrant or attempted processing by BER of lesions normally repaired by NER.

INTRODUCTION

The Base excision repair (BER) pathway is the main mechanism for removal of endogenously generated DNA base damage [1]. BER is initiated by DNA glycosylases that recognise and excise groups of related lesions [2]. There are at least 12 different mammalian DNA glycosylases, of which at least 7 have overlapping specificities towards oxidative DNA damage [3, 4]. *Caenorhabditis elegans* (*C. elegans*) is a multicellular animal that encodes only two DNA-glycosylases: UNG-1 [5, 6] and NTH-1 [7]. *C. elegans* is therefore an attractive system in which to study consequences of BER-deficiency in animals. Furthermore, the strong genetic and mechanistic correlation between stress resistance and longevity in *C. elegans* [8], allows us to probe the contribution of DNA damage, in particular oxidative DNA damage, and its repair to phenotypes associated with oxidative stress in large populations over the entire lifespan.

C. elegans NTH-1, a homolog of *E. coli nth*, was recently shown to have activity against oxidized pyrimidines [7]. A deletion mutant lacking exons 2 through 4, *nth-1(ok724)*, is expected to be a null mutant and has elevated mutant rate [9] but no hypersensitivity to oxidizing agents [7]. The absence of a DNA-glycosylase with specificity towards oxidized purines in

C. elegans is puzzling. Although *C. elegans* NTH-1 appears to have a weak ability to excise one of the major purine oxidation products (8-hydroxyguanine) [7], it seems likely that other DNA repair pathways such as Nucleotide Excision Repair (NER) might contribute to repair of oxidised purines in *C. elegans* as has been shown *in vitro* [10] and in *vivo* in *Saccharomyces cerevisiae* [11]. Genetic studies in *S. cerevisiae* show that NER is the preferred repair pathway for oxidative DNA damage in the absence of BER [12]. The NER pathway is highly conserved and orthologs of the core NER proteins are present in *C. elegans* [13]. XPA is required for formation of the preincision complex [14]. *C. elegans xpa-1* mutants are UV-sensitive [15, 16] and the *xpa-1 (ok698)* mutant has reduced capacity to repair UV-induced DNA damage [13, 17].

Expression profiling in NER-defective mice has revealed gene expression changes associated with segmental progeroid phenotypes [18-20]. For example, the NER-defective *Csbm/m/Xpa*$^{-/-}$ mice show suppression of signaling through the growth hormone (GH)/insulin growth factor 1 (IGF1) pathways and increased antioxidant responses. Similar changes could be induced in wild type mice through chronic administration of a reactive oxygen species (ROS) - inducing agent, suggesting that the transcriptional responses result from defects in transcription-coupled repair of oxidative DNA damage [21].

Although ROS are believed to be a main contributor to the stochastic endogenous DNA damage accumulating with increase age, and BER is the preferred pathway for repair of oxidative DNA damage, similar expression profiling has not been performed in BER defective animals. However, studies in *S. cerevisiae* suggest that mutants in BER as well as NER show global expression profile changes originating from unrepaired oxidative DNA damage after treatment with oxidizing agents [22, 23].

Mutants in DNA glycosylases generally show very mild phenotypes, which has been attributed to the existence of backup enzymes with overlapping substrate specificities. Here we show that compensatory transcriptional responses contribute to maintain wild type phenotypes including lifespan, in the presence of endogenous oxidative stress in DNA repair mutants.

RESULTS

The transcriptional signatures of mixed populations of wild type N2 as well as *nth-1*, *xpa-1*, and *nth-1;xpa-1* mutants were measured using Affymetrix GeneChip *C. elegans* Genome Arrays in well fed animals cultured on plates to avoid stressful growth conditions.

Oxidative stress response and reduced insulin/IGF-1 signaling in *nth-1(ok724)*

Since DNA damage responses often show small changes on the transcriptional level [24], we analysed the gene expression signatures using a fold-change cut-off criterion ≥1.8. We found a high number of differentially expressed transcripts between the N2 reference strain and the *nth-1* mutant considering the unstressed conditions of the animals: 2074 probe sets were differentially expressed ≥1.8 fold (Supplemental Table SI). The low number of transcripts regulated ≥4-fold (185 probe sets) suggests that there is a focused transcriptomic response to loss of the NTH-1 enzyme.

Gene ontology (GO) enrichment analysis revealed that genes involved in determining adult lifespan ($p < 0.007$) were enriched among the regulated genes in the *nth-1* mutant (Figure 1). Of these, 17 are known to act through the insulin/IGF-1 signaling (ILS) pathway. Reduced signaling through the canonical ILS pathway leads to nuclear localisation of the FOXO transcription factor DAF-16 [25]. A total of 84 genes previously identified as downstream targets of DAF-16 (*dod*) [26, 27], were differentially regulated in *nth-1*, of which 67 were not assigned to the aging cluster based on present GO annotation. However, some confirmed targets of DAF-16 (e.g. *hsf-1, hsp-90, hsp-70*) were not differentially regulated, and there was no significant overlap between our dataset and the previously reported *daf-16* dataset [27] (data not shown). Moreover *dao-6*, which is positively regulated by DAF-16 and negatively regulated by DAF-2, was downregulated by 7.7-fold. Thus, the transcriptional changes in the *nth-1* mutant appear not to be dominated by DAF-16. The downregulation of *ins-1* and *ins-7* (2.17 and 3-fold, respectively), two DAF-2 agonists whose expression are repressed by DAF-16, likely reflects negative feedback inhibition of ILS rather than sensory neuronal input to the ILS pathway.

Previous genetic and genomic studies have demonstrated that there is a close interconnection between the ILS and stress-response pathways in *C. elegans* [8, 28]. This is reflected in the *nth-1* dataset: The genes in the aging cluster, as well as individual genes regulated more than 4-fold (Supplemental Table SI), indicate that oxidative stress responses are activated. SOD-3 is a mitochondrial Mn-containing superoxide dismutase [29] and increased expression of *sod-3* has been reported in response to oxidative stress

[30]. *sod-3* is a target of DAF-16, and the well established inverse regulation between *ins-7* and *sod-3* [31] is observed in *nth-1* (-3 and 1.84-fold, respectively). Activation of an oxidative stress response in *nth-1* is further suggested by the upregulation of *gst-4* (2.31-fold), a regulator of SKN-1 which is a transcription factor mediating transcriptional responses to oxidative stress [32]. Regulation of steroid signaling and stress responses are also reflected in the second GO enriched cluster, proteolysis ($p < 0.01$) (Figure 1).

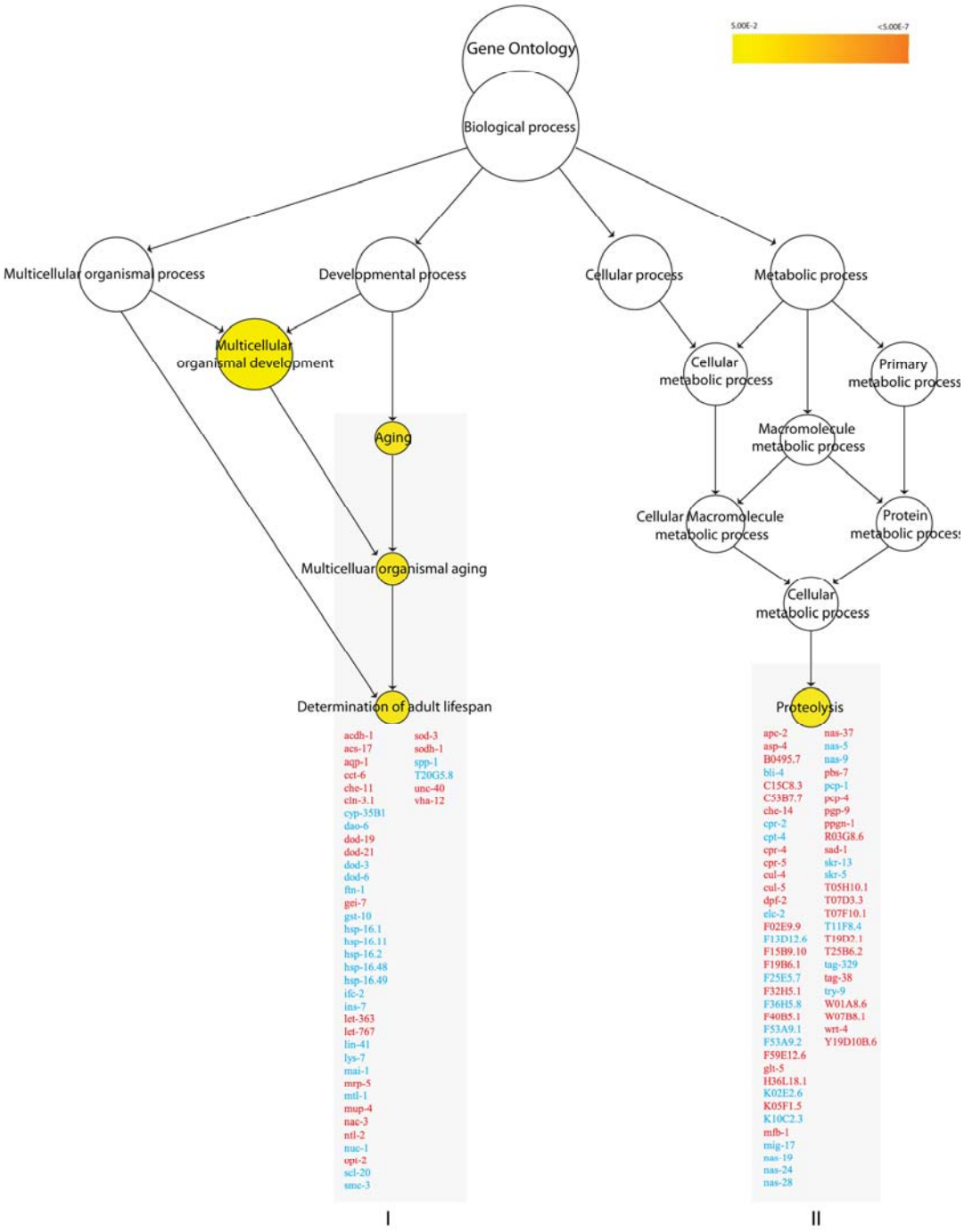

Figure 1. Overrepresented biological processes in N2 vs. *nth-1*. Enriched biological processes in *nth-1* vs. N2 are Aging *($p < 0.007$)* and Proteolysis *($p < 0.01$)*. The Aging cluster contains 17 genes involved in ILS signaling, including *ins-7* and *sod-3*. Genes responding to stress and steroid signaling are found in the Proteolysis cluster. Genes in red and blue are found to be upregulated and downregulated, respectively.

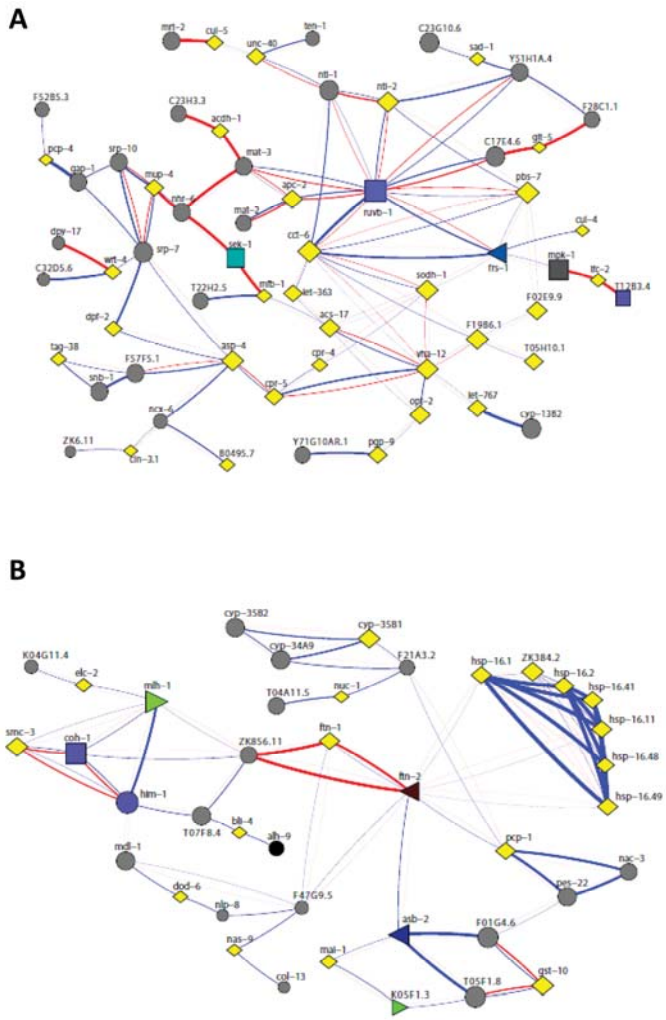

Figure 2. Network analysis revealed a close interconnection between the two enriched clusters in *nth-1*. (**A**) Functional interactions among upregulated genes in the two clusters was analysed using FunCoup [54]. A network of 97 most probable links between 95 genes was returned, involving 31 of the 58 regulated genes (12 and 19 from cluster I and II, respectively). (**B**) Network analysis of the 45 downregulated genes resulted in a network of 79 most probable links between 71 genes from both clusters.

A search for functional interactions among upregulated genes in the two clusters using the online functional interaction browser FunCoup revealed a close interconnection between the two enriched clusters involving 31 of the 58 regulated genes (12 and 19 from cluster I and II, respectively) (Figure 2A). The expression of the CeTOR (let-363) kinase is upregulated in *nth-1* (2.33-fold), possibly indicating activation of a survival response to stress. The TOR pathway controls protein homeostasis and contributes to longevity, and the network analysis indicates that TOR might connect the two clusters via the AAA+ ATPase homolog RUVB-1, a component of the TOR pathway [33]. Direct protein-protein interactions involving RUVB-1 have been demonstrated with several upregulated genes in both enriched GO clusters.

The protein-interaction network (Figure 2A) suggests that the transcriptional changes may also involve regulation of the redundant activities of the conserved p38 and JNK stress-activated protein kinase pathways: MFB-1, for example, directly interacts with SEK-1, a MAPK kinase required for germline stress-induced cell death independent of the CEP-1 (*C. elegans* p53) DNA damage response [34]. SEK-1 is also required for nuclear localisation of DAF-16 in response to oxidative stress [35]. It was suggested that oxidative stress mediates regulation of DAF-16 through activating the p38 signal transduction pathway upstream of DAF-16. Therefore, regulation of DAF-16 target genes in *nth-1* is consistent with activation of an oxidative stress response. Alternatively, the regulation of DAF-16 targets could be secondary to *aqp-1* upregulation. Aquaporin-1, a glycerol channel protein, was recently demonstrated to modulate expression of DAF-16-regulated genes and suggested to act as a feedback regulator in the ILS pathway [36]. There is a strong upregulation of *aqp-1* in *nth-1* (31-fold). Moreover, 6 out of 7 genes negatively regulated by AQP-1 are repressed in *nth-1* (Supplemental Table SII).

Network analysis of the 45 downregulated genes resulted in a network involving 71 genes from both clusters (Figure 2B). The pronounced downregulation of genes specifically responding to exogenous oxidative and heat stress (such as the *hsp-16* family, *ftn-1* and *gst-10*, *lys-7*, *mtl-1*) and anti-microbial immunity (several c-lectins, *cpr-2*, *ilys-3*, *abf-2*, *cnc-7*) in the *nth-1* mutant suggests that a specific response to endogenous stressors is triggered. Hence, loss of BER in *C. elegans* appears to induce transcriptional responses involving similar pathways as those regulated in mammalian NER mutants [19].

Shared transcriptional responses in *nth-1* and *xpa-1* mutants

To experimentally validate whether there is similarity between the transcriptional programs associated with loss of BER and NER capacity in *C. elegans*, we collected the expression profile of the *xpa-1(ok698)* mutant. In *xpa-1*, we identified 2815 differentially expressed transcripts having a fold-change of ≥1.8 (Supplemental Table SIII).

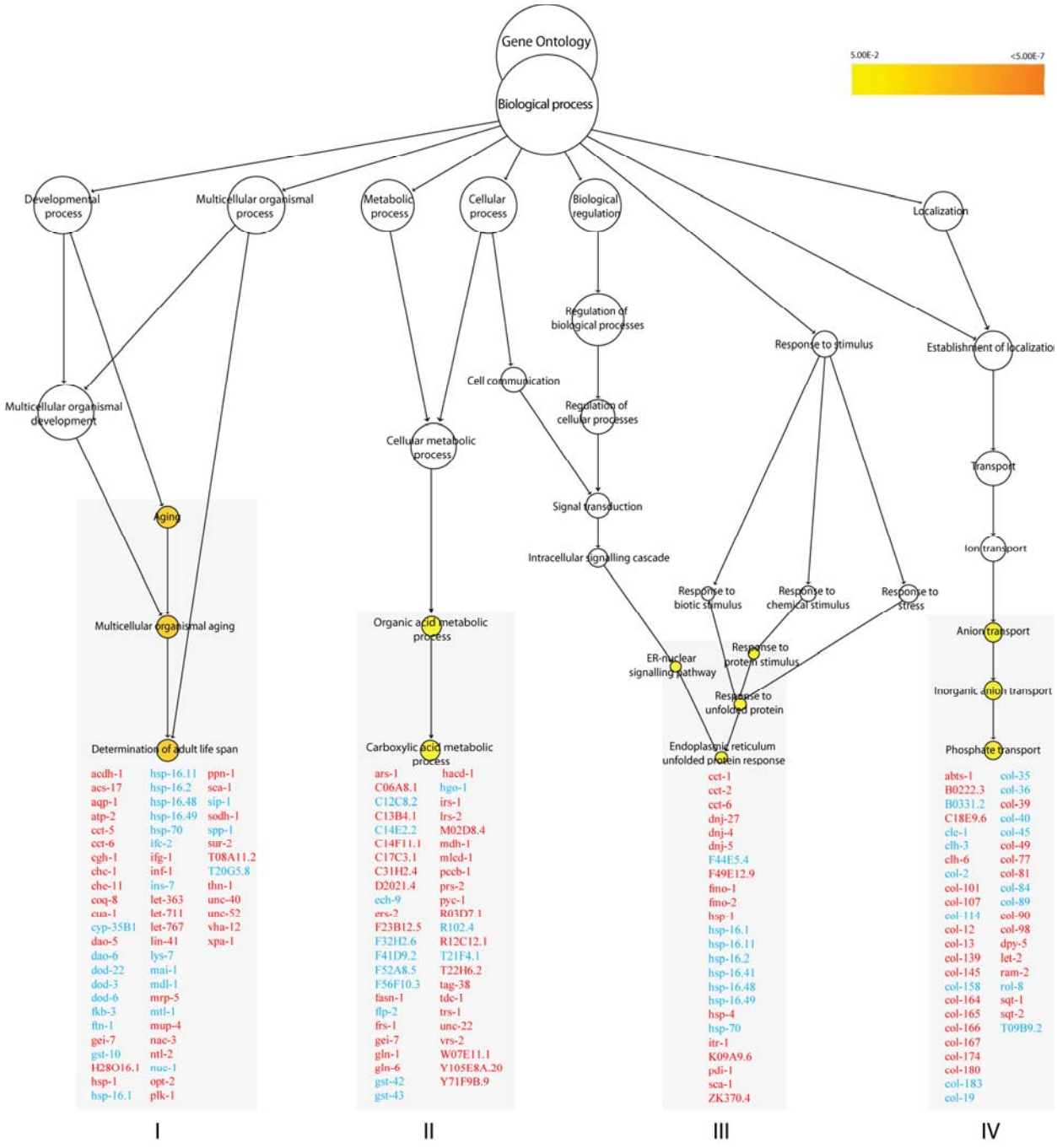

Figure 3. GO enrichment clusters in *xpa-1*. Genes that respond to oxidative stress and redox homeostasis are found in the enriched biological processes in *xpa-1* vs. N2. Aging *($p < 0.0007$)*, regulation of carboxylic acid metabolism ($p < 0.03$), ER unfolded protein response ($p < 0.05$) and phosphate transport ($p < 0.02$). Genes in red and blue are found to be upregulated and downregulated, respectively.

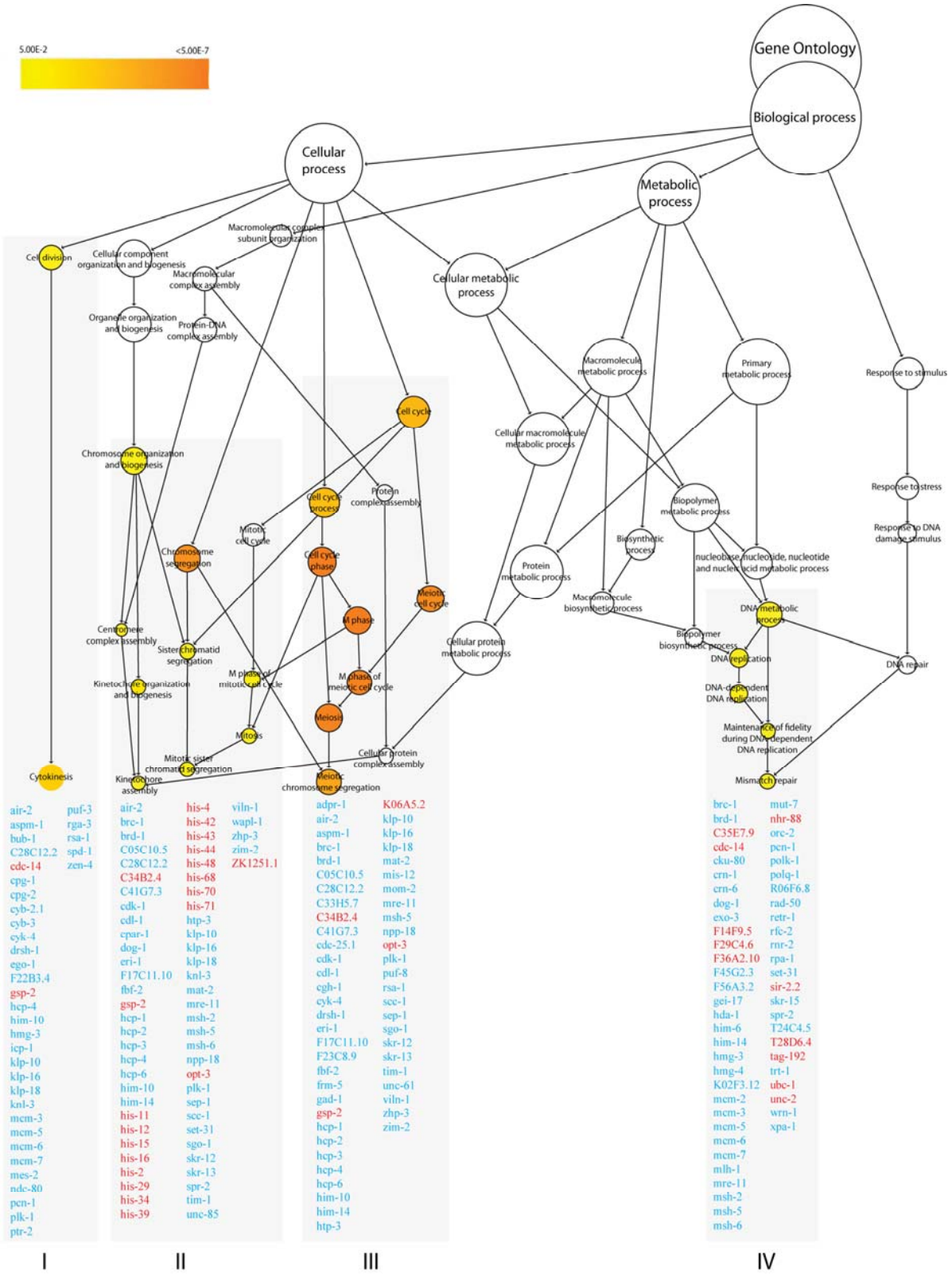

Figure 4. GO enrichment clusters in *nth-1;xpa-1*. The transcriptional response in the double mutant *nth-1;xpa-1* is dominated by genes involved in cell-cycle regulation (clusters I-III) and DNA repair (cluster IV). Cluster I ($p < 0.003$) and II ($p < 0.01$) contain genes that function in mitosis-related processes. Cluster III ($p < 0.00001$) reflect regulation of progression through meiosis. Genes involved in DNA repair and DNA damage checkpoint pathways in cluster IV ($p < 0.02$) are downregulated. Genes in red and blue are found to be upregulated and downregulated, respectively.

GO enrichment analysis revealed four significantly regulated clusters in *xpa-1* (Figure 3). The GO process determination of adult lifespan ($p < 0.0007$) was shared with *nth-1* (Figure 1), and 67% (28 out of 42) of the individual genes in this cluster in *nth-1* were shared with *xpa-1*. In *xpa-1*, genes that respond to oxidative stress and redox homeostasis are not only represented in the "aging" cluster, but are also found in the clusters containing genes involved in the ER unfolded protein response ($p < 0.05$) and regulation of carboxylic acid metabolism ($p < 0.03$). Network analysis of the 57 downregulated genes within the enriched clusters resulted in a network resembling that of nth-1 (Supplemental Figure S1). Thus, qualitatively similar responses were activated to compensate for the loss of NTH-1 or XPA-1. Regression analysis using the 1.8-fold-change data confirmed the similarity of the *nth-1* and expression profiles ($R_2 = 0.96$). However, there is stronger modulation of gene expression in *xpa-1* compared to *nth-1*, with an increased number of transcripts with higher fold-change; e.g. expression of *ins-7* (8.8-and 3-fold), *aqp-1* (34.8- and 31-fold, respectively), and *hsp-16.49* (-15.99 and -5.58- fold) in *xpa-1* and *nth-1*, respectively (Supplemental Tables SI and SIII).

Somatic preservation in *nth-1;xpa-1*

Genes regulating adult lifespan were not among the four enriched GO processes identified from the 2787 regulated probe sets with fold-change ≥1.8 (1225 up and 1562 down) in *nth-1;xpa-1* (Figure 4 and Supplemental Table SIV). Instead, the transcriptional response was dominated by genes involved in cell-cycle regulation (clusters I-III) and DNA repair (cluster IV). Cluster I ($p < 0.003$) and II ($p < 0.01$) contain genes that function in mitosis-related processes such as chromosome segregation, mitotic spindle assembly and stability, and replication licensing. Only 2 out of 36 genes in cluster I are upregulated. In contrast, 15 of the 64 genes present in cluster II are upregulated and most encode histone genes. Cluster III ($p < 0.00001$) share many genes with cluster I and II but reflect regulation of progression through meiosis.

Genes involved in DNA repair and DNA damage checkpoint pathways are enriched in Cluster IV ($p < 0.02$). Naively, it could be expected that the double mutant would compensate for loss of integrity of two DNA repair pathways by upregulating alternative DNA repair modes. However, the opposite seems to be the case. Several mismatch repair, homologous recombination (HR), non-homologous end-joining (NHEJ), and DNA damage checkpoint genes, such as the *C. elegans* homolog of BRCA1 (*brc-1*) and its associated proteins, *brd-1* and *dog-1*, are downregulated (Table 1). Many uncharacterized genes that have previously been identified in screens for genes that result in mutator phenotypes when depleted by RNAi [37, 38] were also suppressed in the *nth-1;xpa-1* mutant. Network analyses illustrate close interrelation of clusters I through IV also on protein level returning protein-protein interactions between 157 of the 212 genes in all clusters (data not shown).

Suppression of the Aurora-B kinase and Polo-like kinase 1 regulatory network in *nth-1;xpa-1*

The GO analysis suggests that the double mutant differs from either single mutant. Linear regression analysis comparing the overlapping transcripts in the ≥1.8-fold-change lists from *nth-1;xpa-1* and *xpa-1* confirmed this difference (R2 = 0.12) whereas the single mutants show significantly stronger correlation ($R_2 = 0.94$). Principal Component Analysis (PCA) on the entire dataset (Figure 5A) confirms that the overall expression profiles of the single mutants cluster together and therefore resemble each other but, although *nth-1;xpa-1* clusters separately from the wild type, it seems to be in closer proximity to it than to either single mutant. Hierarchical clustering confirmed the closer relationship between *nth-1;xpa-1* and the wild type (Supplemental Figure S2). Hierarchical clustering of the mutants only revealed even more clearly that the single mutants are more similar to each other than either are to the double mutant. Several transcripts have opposite regulation, most notably in *xpa-1* and *nth-1;xpa-1* (Figure 5B). DNA repair and DNA damage response genes are prominent among the genes regulated in an opposite direction (a selection is presented in Table 1).

Polo-like kinase 1 (PLK-1), which is upregulated in *xpa-1* (1.97-fold) but repressed in *nth-1;xpa-1* (-2.11-fold), has emerged as an important modulator of DNA damage checkpoints [39, 40]. Moreover, Aurora B kinase (*air-2*) is downregulated (-1.83-fold), and an inhibitor of AIR-2 activation, gsp-2, is one of the few upregulated genes in *nth-1;xpa-1*. Several other components of AIR-2 and PLK-1 networks are represented in the enriched GO clusters in the double mutant (Figure 4). Moreover, the transcriptional changes observed in *nth-1;xpa-1* involved several genes that are validated interactors of AIR-2 and PLK-1. The direction of the expression changes suggests that there is a concerted response that suppresses AIR-2 and PLK-1 signaling networks in the double mutant (Figure 6) that are consistent with published literature evidence: Plk-1 stimulates the activation of Cdk-1, several cyclin

B proteins and a G2/M specific cyclin A through Cdc-25.1 [40]. The inner centromere protein (INCENP), ICP-1, coordinates cytokinesis and mitotic processes in the cell and integrates the PLK-1 and AIR-2 signaling at kinetochores. AIR-2 and PLK-1 regulate mitosis and cytokinesis through CYK-4 and ZEN-4 [41]. Downregulation of MCM2-7 could prevent firing of dormant replication origins which are often used when the transcriptional machinery is blocked or otherwise impaired [42]. Hence, the suppression of DNA metabolism suggested by the transcriptional signature reflects a concerted response. In summary, there seems to be a two-tiered compensatory response to loss of DNA repair in *C. elegans*: While lack of either BER or NER results in activation of genes responding to endogenous stressors and suppression of ILS, lack of both BER and NER shifts the transcriptional response to reduction of proliferation and somatic preservation through modulation of AIR-2 and PLK-1 signaling networks.

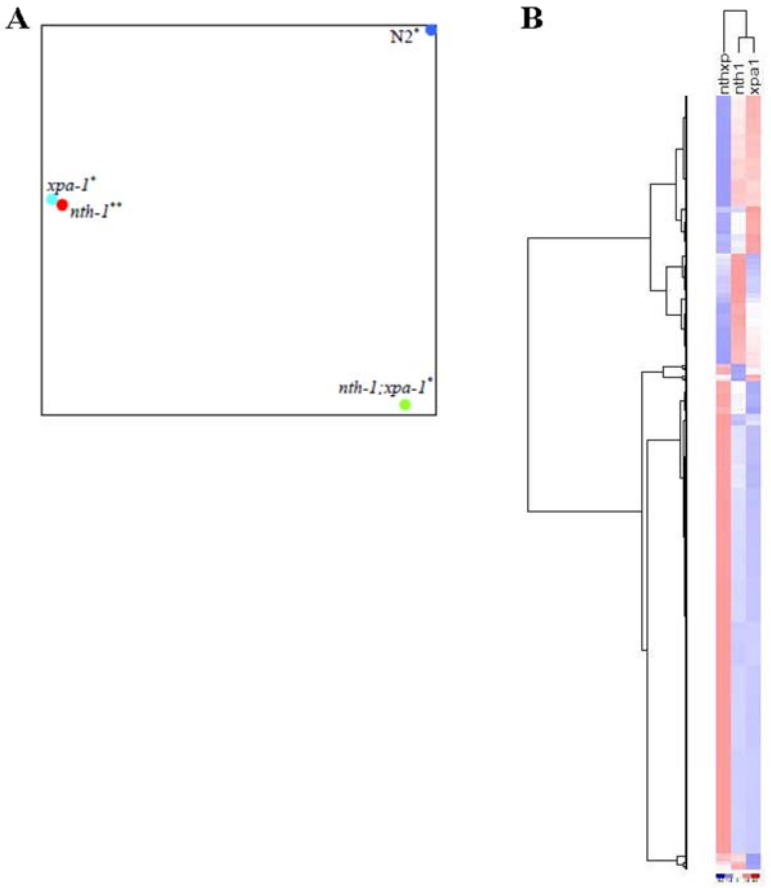

Figure 5. Comparative analyses of transcriptomes in DNA repair mutants. (**A**) The distance between respective mutants denoting the similarities or dissimilarities between *nth-1* (red circle), *xpa-1* (light blue circle), *nth-1;xpa-1* (green circle) and wild-type (blue circle) is shown using PCA. (**B**) Separation of the different mutant sample groups using Hierachical clustering.

Table 1. Regulation of DNA repair and DNA damage response genes in DNA repair mutants*

pathway		Gene[#]	Fold-change[+]		
			nth-1	*xpa-1*	*nth-1;xpa-1*
DNA repair	BER/NER	*exo-3*			-2,38
	MMR	*exo-1*			-2,03
		mlh-1		2,83	-2,23
		msh-2		1,83	-1,94
		msh-6		2,33	-1,9
	HR	*dna-2*		1,85	-2,43
		rad-50			-1,85
	NHEJ	*mre-11*			-1,94
		cku-80			-2,1
	DSB	*cnb-1*			2,19
		crn-1			-1,93
		polk-1			-2,21
		polq-1		2,45	-2,61
	Helicases	*dog-1*		1,89	-1,91
		him-6		2,95	-2,15
		wrn-1			-1,97
	Other	*rpa-1*			-2,03
		pcn-1			-2,24
		dpl-1		2,06	-2,01
		rfc-2			-1,97
DNA Damage Response/Cell Cycle		*air-2*		2,09	-1,9
		ani-2		1,82	-2,21
		brc-1			-1,85
		brd-1			-1,99
		C16C8.14		1,94	2,16
		cdc-14			-2,16
		cdc-25.1			-1,88
		gst-5			-2,26
		hil-1		-2,08	2,47
		hsr-9		1,83	-1,98
		K08F4.2			-2,19
		lin-35			-1,9
		mdf-1			-1,96
		pme-5	1,96	2,69	-1,95

*Gene classifications were determined based on previous analyses in references [54] and from information presented in Wormbase (www.wormbase.org)

[#] A selection of DNA repair and DNA damage response genes regulated in *nth-1;xpa-1*

[+] Fold-changes calculated from the comparative analyses presented in Supplemental Tables SI, SIII and SIV

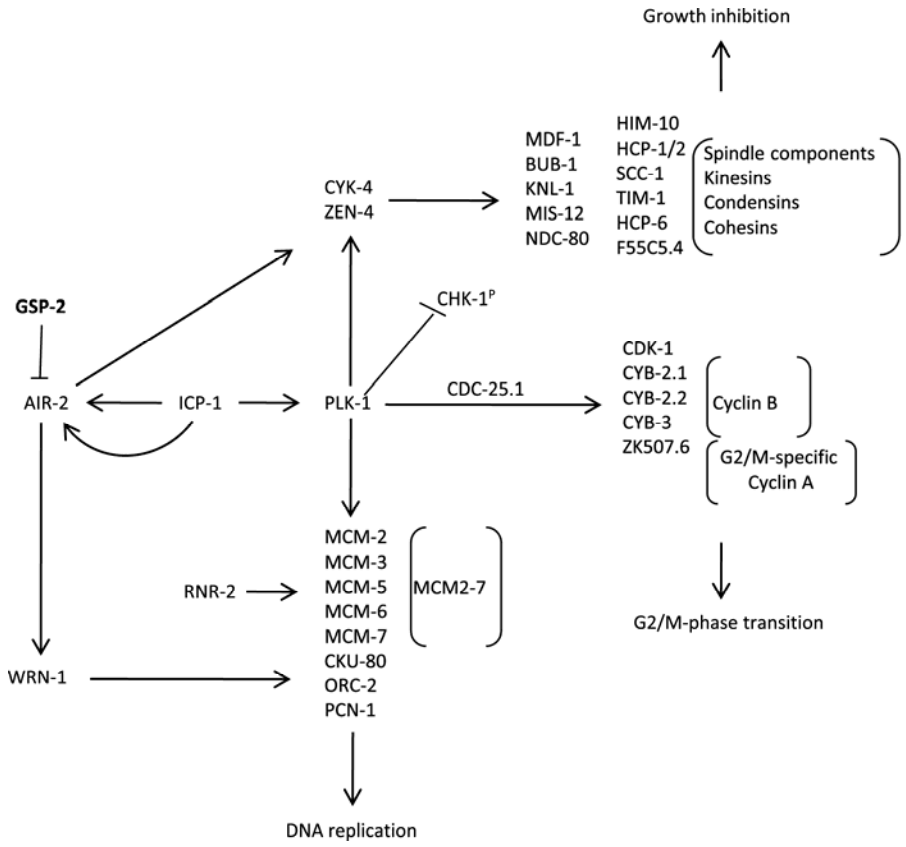

Figure 6. Somatic preservation through modulation of AIR-2 and PLK-1 signaling networks in *nth-1;xpa-1*. Genes encoding proteins known to stimulate AIR-2 and PLK-1 signaling are downregulated in *nth-1;xpa-1*: Plk-1 is known to stimulate activation of CDK-1, several cyclin B proteins and a G2/M specific cyclin A through CDC-25.1. Furthermore, PLK-1 and AIR-2 signaling coordinates cytokinesis and mitotic signaling at kinetochores via in the inner centromere ICP-1, regulates mitosis and cytokinesis through CYK-4 and ZEN-4, and could prevent firing of dormant replication origins via **d**ownregulation of MCM2-7. An inhibitor of AIR-2 activation, GSP-2, is one of the few upregulated genes**.**

Depletion of NTH-1 and XPA-1 induces oxidative stress responses

Transcriptomic profiling strongly indicates that the *nth-1* and *xpa-1* mutants experience oxidative stress. To experimentally validate whether loss of NTH-1 and XPA-1 induces oxidative stress, we took advantage of the established reporter strain CL2166, which expresses green fluorescent protein (GFP) under the control of the glutathione-S-transferase GST-4 promoter [32]. *gst-4* expression is upregulated in both *nth-1* and in *xpa-1* (2.31, and 2.01-fold respectively). Whereas GFP is normally expressed in hypodermal muscle, GFP-fluorescence increases in the body wall muscles and translocates to the intestinal nuclei upon oxidative stress

As expected, paraquat, which generates superoxide *in vivo*, increases the average number of GFP positive intestinal nuclei up to 46 compared to 15 in untreated animals ($p < 0.001$). Depletion of NTH-1 or XPA-1 by RNAi significantly increased the number of foci to 26 and 25, respectively ($p < 0.001$) (Figure 7), thus demonstrating that even transient depletion of NTH-1 or XPA-1 induces oxidative stress responses. Co-depletion of NTH-1 and XPA-1 did not increase the number of intestinal GFP-positive foci. The *gst-4*::GFP reporter assay therefore experimentally validated the high throughput genomic results and confirmed that loss of NTH-1 or XPA-1, but not both, leads to oxidative stress and activation of oxidative stress responses.

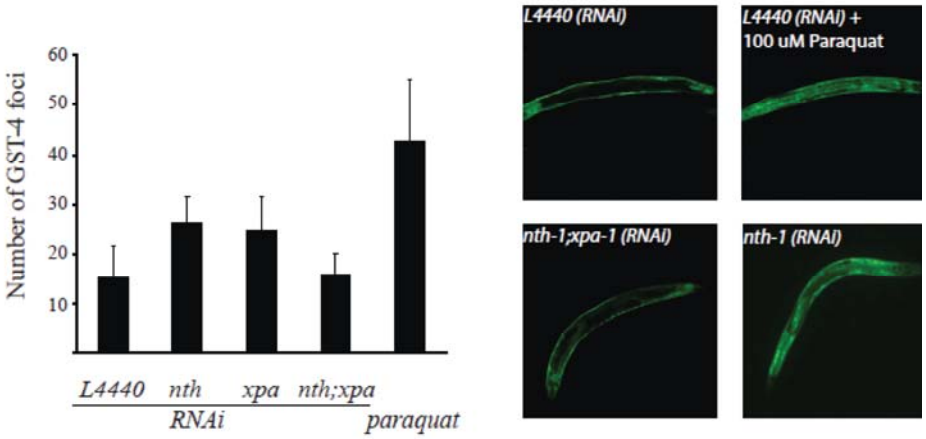

Figure 7. Oxidative stress is induced upon depletion of NTH-1 or XPA-1. The CL2166 reporter strain harbouring a GFP under the control of the *gst-4* promoter was used to determine whether reduction of BER or NER, via *nth-1(RNAi)* and *xpa-1(RNAi)* respectively, or both pathways induces oxidative stress. A significant increase in GST-4 foci compared to the empty vector control (*L4440* (n = 97)) was observed in animals treated with RNAi against NTH-1 (n = 57) or XPA-1 (n = 95) *(p<0.0001)* using Student's *t*-test). Co-depletion of NTH-1 and XPA-1 (n= 46) did not give more GST-4 positive foci (*p* = 0,507). GST-4 positive foci induced by paraquat (100 µM) was included as a positive control (n = 50).

The transcriptional changes do not protect against exogenous acute stress

The expression profiling indicated that the transcriptional responses in the single-mutants are aimed at compensating for oxidative stress resulting from DNA-repair deficiency. The responses appear to be selectively tuned to compensate for endogenous stress. The down-regulation of other stress induced factors, such as the *hsp-16* family, may serve to prevent unsolicited activation of a full-blown stress response. Thus, we would not expect the DNA repair mutants to show resistance to oxidizing agents which is correlated with reduced ILS in *C. elegans* [8, 30]. In agreement with previous reports, neither *xpa-1* [43], nth-1 [7] nor *nth-1;xpa-1* were hypersensitive to paraquat (data not shown). However, all mutants showed mild sensitivity to an acute exposure to another superoxide generating agent, juglone (Figure 8A) and mild heat-shock (data not shown). Hence, the upregulation of oxidative stress responses do not confer resistance to acute exogenous stress. These phenotypes are consistent with downregulation of genes responding to exogenous stressors as observed.

Loss of NTH-1 restores normal lifespan in *xpa-1*

Reduced ILS induces longevity in *C. elegans* [44], but reduced ILS is also seen in segmental progeroid NER defective mice [21]. This apparent paradox can be interpreted as the reduced ILS in the DNA repair defective mice is part of a compensatory attempt to extend lifespan in organisms suffering from DNA damage associated stress. Thus, we were interested to test whether the reduced ILS in *nth-1* and *xpa-1* observed here was accompanied by reduced lifespan – or whether the compensatory response was sufficient to sustain normal lifespan. The lifespan of nth-1 was indistinguishable from the wild type, as was recently shown [7], whereas the *xpa-1* mutant displayed reduced lifespan compared to the wild type (mean survival of 14.5 and 17.3 days, respectively) (Figure 8B). In *C. elegans* therefore, as in mice, the challenges that loss of NER poses to the organism is more severe than loss of a single DNA-glycosylase. Our results demonstrate that this difference in challenge can be read out as a stronger activation of the antioxidant defense and reduction in ILS.

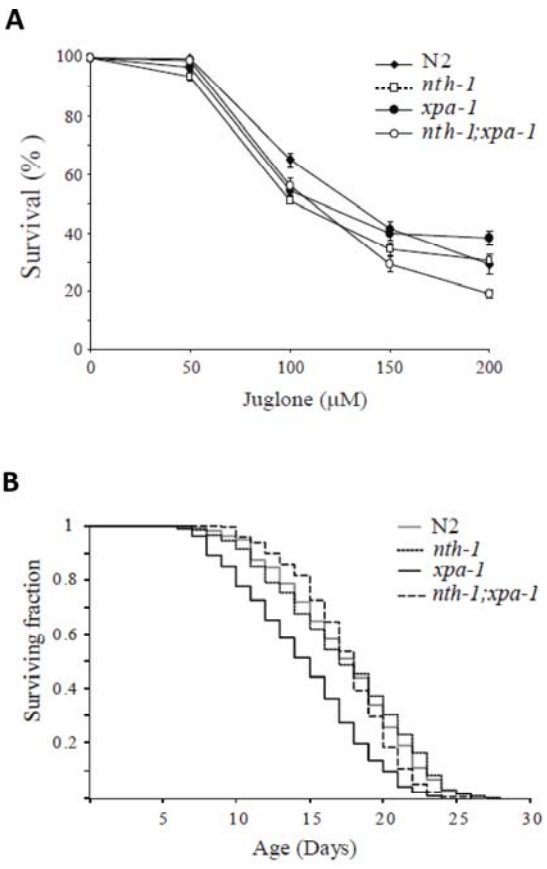

Figure 8. Compensatory responses specific for endogenous stressors. (**A**) Increase in the oxidative stress response do not confer resistance to juglone. Viability was scored as touch-provoked movement after 24 hour recovery from one hour exposure of young adults to juglone. Mean survival (+/- standard error of the mean) relative to untreated control was calculated from five independent experiments comprising a total of 250-350 animals. (**B**) Lack of *nth-1* rescues the lifespan of an *xpa-1* mutant. Synchronized L4 larvae were placed on NGM plates at t = 0, incubated at 20°C, and transferred daily to fresh plates during the egg-laying period. The worms were monitored daily for touched-provoked movement; animals that failed to respond were considered dead. The *xpa-1* mutant shows a reduced lifespan compared to *nth-1* and *nth-1;xpa-1* and wild type, N2.

The *nth-1;xpa-1* double mutant has a more profound DNA repair defect and is expected to be unable to repair a much wider spectrum of DNA lesions. If the accumulation of DNA damage itself is the bigger lifespan reducing challenge in xpa-1, we would expect nth-1;xpa-1to be more severely affected. Interestingly, normal lifespan was restored in *nth-1;xpa-1* with a mean survival of 17.4 days. One possible interpretation of these results is that the oxidative lesions most relevant for aging are those that are normally repaired by NER, but are attempted processed by BER in the absence of the preferred repair pathway.

DISCUSSION

Mutants in DNA glycosylases generally have weak phenotypes. This has been explained by the existence of backup enzymes with overlapping substrate specificities. Here we present data that reveal additional explanations to how wild type phenotypes and lifespan are maintained in animals that lack a DNA glycosylase.

Oxidative stress induced in DNA repair mutants

Here we present the first comprehensive report describing compensatory transcriptional responses to loss of base excision repair genes in animals. Using a well established transgenic reporter assay, we show that transient depletion of NTH-1 and XPA-1 by RNAi induces oxidative stress, thus it seems likely that this initiates transcriptome-modulation in the mutants. We show that lack of the NTH-1 and XPA-1 enzymes are accompanied by upregulation of oxidative stress responses tuned towards endogenous stressors. This is in agreement with identification of a focused compensatory response to BER intermediates (AP-sites and strand breaks) previously shown in *S. cerevisiae*, where the transcriptional responses differed from the common environmental stress response or the DNA damage signature [45]. A DNA-damage dependent ROS response to unrepaired oxidative DNA damage was previously demonstrated in *S. cerevisiae* BER and NER mutants [46]. Interestingly, no indication of oxidative stress or increased expression of oxidative stress response genes was observed in a mutant lacking both NTH-1 and XPA-1. This transcriptomic shift argues against a DNA-base damage dependent activation of oxidative stress responses, but instead indicates that the DNA repair enzymes mediate signaling to activate stress response pathways. Although the upstream signaling events in the *nth-1;xpa-1* double mutant remain to be elucidated, the modulation of AIR-2 and PLK-1 interaction networks may be a consequence of absence of DNA repair enzyme-mediated signaling of transcription blocking lesions. Alternatively, the extensive new synthesis of histone genes suggests that signaling involves chromatin dynamics in the absence of the global genome damage binding proteins, NTH-1 and XPA-1.

The biological significance of transcriptome modulation seen here is confirmed by the DNA repair mutants showing a mild sensitivity to oxidizing agents. It seems likely that the downregulation of the *hsp-16* family and *ftn-1* contributes to the higher sensitivity to juglone in *xpa-1* and *nth-1*, particularly as it is unlikely that a short acute exposure to oxidizing agents (or heat-stress) may

lead to DNA-damage mediated toxicity on organismal level.

Conserved compensatory responses to BER and NER deficiency

Few systematic studies have been performed to look at transcriptomic changes in BER mutant animals and none, to the best of our knowledge, have compared mutants in BER and NER.

A study on gene expression profiling in BER- or NER-defective mutant *S. cerevisiae* showed transcriptional changes in mutants defective in both pathways after treatment with hydrogen peroxide [22], but not in the double mutant. Instead, transcriptome changes in the BER/NER defective strain were already elicited from unrepaired spontaneous DNA damage [23]. To test the generality of our finding, we re-analyzed the baseline data sets from *S. cerevisiae* BER (Ntg1, Ntg2, and Apn1 deficient), NER (Rad1 deficient) and BER/NER defective mutants. We performed GO enrichment analysis on expressed transcripts in the individual strains (Supplemental Table SV). This analysis showed that BER-defective cells had few expressed transcripts and only one enriched GO process, DNA replication ($p < 0.05$). Informative enriched GO processes found only in the NER defective strain include transcription regulation, ubiquitin dependent protein degradation, sister chromatid segregation, and cell communication ($p < 0.01$). The BER/NER and NER defective cells share many enriched GO clusters and show 38% overlap of individual expressed transcripts. Enriched GO processes found only in the BER/NER mutant include DNA repair, DNA packaging, response to DNA damage stimulus, and cell-cycle checkpoint. Regulation of RNA polymerase II transcription was not enriched in the BER/NER mutant. Therefore, the main conclusions drawn here from BER, NER and BER/NER deficient *C. elegans*, resemble those previously seen in *S. cerevisiae* [22, 23, 45]: i) BER mutants show transcriptomic changes. ii) Loss of NER induces more substantial transcriptional responses than BER involving modulation of RNA metabolism and regulation of transcription iii) Loss of BER in the NER mutant shifts the response to regulate processes that maintain DNA integrity.

Reduced mean lifespan in *xpa-1(ok698)*

The first *xpa-1* mutant identified, *rad-3(mn159)*, was reported to have a near-normal lifespan [15] but there are conflicting reports on the lifespan of *xpa-1(ok 698)* allele ranging from normal [43] to a maximum lifespan of 15 days compared to 25 days in the wild type [17]. Here, we show a moderate reduction of lifespan in *xpa-1*. We did therefore not anticipate that the XPA-1 mutant would display a transcriptional profile resembling that of the segmental progeroid NER defective mice [19]. Nevertheless, the reduced lifespan is entirely consistent with the transcriptional changes observed. A recent transcriptomic signature of $Xpa^{-/-}$ mouse dermal fibroblasts shows that suppression of ILS and activation of oxidative stress responses is also seen in DNA repair mutants that do not exhibit accelerated aging [47]. In support of this, GO enrichment analysis, performed as part of the present study, on the differentially expressed genes in $Xpa^{-/-}$ mice [21] showed enrichment of genes that regulate lifespan. Hence, the transcriptomic changes in NER mutants are conserved.

However, the consequences of loss of XPA-1 appear more severe in *C. elegans* compared to mice, both with respect to transcriptional regulation and lifespan. This might indicate that *C. elegans* XPA-1 contributes to repair of spontaneous DNA damage. The 13-fold elevated mutation accumulation rate in *xpa-1* compared to 7-fold in *nth-1* [9], supports this possibility.

CONCLUDING REMARKS

Based on a large body of evidence indicating that persistent transcription-blocking DNA damage cause attenuation of ILS and activation of oxidative stress responses [18-20, 47], it is reasonable to speculate that the transcriptome modulation in the *xpa-1* mutant reflects accumulation of transcription blocking DNA lesions. That similar changes are seen in the *nth-1* mutant suggests that such transcriptomic shifts may be a general strategy for survival in DNA repair mutants. Since BER is the main pathway for repair of endogenous oxidative lesions, this lends further support to the notion that oxidative DNA damage contributes to these phenotypes. However, few known BER substrates are recognized as being transcription blocking and cyclopurines, that are often mentioned in this context [47], are NER substrates [48]. The qualitatively different responses in the double mutant support a model where the NTH-1 and XPA-1 enzymes themselves take part in the signaling events that result in activation of responses tunes to compensate for endogenous stress and suppression of ILS. We hypothesize that binding or inefficient processing of oxidative damage relevant to aging in the absence of the preferred repair pathway leads to formation of transcription blocking structures or signaling inter-mediates. The restoration of normal lifespan upon

deletion of NTH-1 supports this hypothesis and strongly suggests that inefficient BER-mediated processing of lesions normally repaired by NER, results in intermediates that pose a lifespan-reducing challenge.

MATERIALS AND METHODS

Strains and culture conditions. All strains were maintained at 20°C as described [49]. The wild-type Bristol N2, *nth-1(ok724)*, *xpa-1(ok698)* and the transgenic strain CL2166 (*dvIs19[pAF15(gst-4::GFP::NLS*) were all kindly provided by the Caenorhabditis Genetic Center (University of Minnesota, St Paul, MN, USA). The double mutant *nth-1(ok724)*; *xpa-1(ok698)* was generated for this work. All strains were backcrossed 3-4 times immediately ahead of the experiments.

RNA isolation and microarray processing. Mixed stage populations of N2, *xpa-1*, *nth-1* and *nth1;xpa-1* were reared at 20°C on HT115(DE3)-seeded on NGM plates (30 plates per replicate, 3 replicates per strain) until the nematodes had cleared the plates of food. Worms were washed off with S-medium, left to digest remaining food in the gut, and washed 3 times before pelleting and suspended in TRIZOL and frozen at -80°C. Total RNA isolation was then performed by standard procedures (Invitrogen). Synthesis of double stranded cDNA and Biotin-labeled cRNA was performed according to manufacturer's instructions (Affymetrix, Santa Clara, CA, US). Fragmented cRNA preparations were hybridized to the Affymetrix GeneChip *C. elegans* Genome Arrays on an Affymetrix Fluidics station 450. Data deposit footnote: GSE16405.

Data and statistical analysis. The processing and primary data analysis was performed in DNA-Chip Analyzer (dChip) (http://biosun1.harvard.edu/complab/dchip/) where normalization (invariant set), model-based expression correction (PM-only model), comparative analysis, PCA and Hierachical clustering was conducted. XLStat (Excel) was used for linear regression analysis. Enriched GO clusters were analysed using Cytoscape [50], in conjunction with the plug-in system BiNGO [51] in addition to DAVID (http://niaid.abcc.ncifcrf.gov) [52, 53]. The Hyper-geometric Test with Benjamini-Hochberg False Discovery Rate Correction was chosen for both the analyses [51]. Functional interaction networks were generated using the online browser FunCoup [54].

gst-4::GFP expression. RNAi feeding constructs in the pL4440 vector harbouring the NTH-1 and XPA-1 open reading frames were generated by Gateway Technology and transformed into *E. coli* HT115(DE3). NGM plates containing 2 mM IPTG seeded with bacteria expressing the empty vector control L4440 or *nth-1*(*RNAi)*, *xpa-1(RNAi)* individually or in combination were activated at 37°C for one hour and left to cool to room temp before the CL2166 reporter strain was added. Plates containing 100 µM paraquat (Sigma) were used as positive control. All plates were incubated at 20°C for 2 days before quantification of GST-4 foci on a Nikon eclipse Ti microscope.

Sensitivity to oxidising agents. The sensitivity to the superoxide-generating compound juglone (Sigma) was performed as previously described [55]. Briefly, young adults were exposed to juglone dissolved in M9 buffer for 1 hour in liquid culture. Viability was scored as touch-provoked movement after a 24h recovery period at 20°C on NGM plates seeded with OP50.

Lifespan determination. Assessment of lifespan was performed essentially as described [56]. Briefly, synchronized L4 larvae were placed on NGM plates at t = 0, incubated at 20°C, and transferred daily to fresh plates during the egg-laying period. The worms were monitored daily for touched-provoked movement. Triplicates comprising 10 plates containing at least 10 worms per plate were performed for each strain. Kaplan-Meier survival distributions were generated and Wilcoxon's log rank test was used to assess significance.

Comparisons with published microarray and Real-Time PCR data. Our datasets were compared to data from van der Pluijm et al. [21]: Significantly differentially expressed transcripts found in $Xpa^{-/-}$ compared to wild type mice were extracted and translated into corresponding *C. elegans* orthologs (using NetAffx, http://www.affymetrix.com/analysis/index.affx). These orthologous set of genes were analysed using Cytoscape [50] to find enriched GO Biological Processes.

Next, we compared our results to datasets generated by Evert et al. from untreated wild type, BER, NER and BER/NER *S. cerevisiae* mutants [51]. Cytoscape was used in order to get a comprehensive overview of enriched Biological Processes in each individual sample group. Also, using dChip, expressed transcrips from each sample group were re-analysed in a comparative analysis giving a list of differentially expressed transcripts with a fold-change ≥2 between wild type and mutant cells. In dChip, replicates were combined and a mean signal value was calculated prior to the comparative analysis. These fold-change lists were then imported into Cytoscape for GO enrichment analysis.

Finally, we extracted genes found to be significantly differentially expressed in the *aqp-1* compared to the wild type in a Real-Time PCR data set from a recent paper by Lee et al. [51] and compared these to our data set.

ACKNOWLEDGEMENTS

We are grateful to Ian M. Donaldson, Sabry Razik and Garry Wong for helpful suggestions and the Nordforsk *C. elegans* network for support. The Affymetrix service was provided by the Norwegian Microarray Consortium (NMC) at the national technology platform, and supported by the functional genomics program (FUGE) in the Research Council of Norway. The research council of Norway for funding (JML, HN), Univesity of Oslo (HN, TR, ØF, HK), EMBIO (ØF). IB was the recipient of an Erasmus exchange grant.

CONFLICT OF INTERESTS STATEMENT

The authors of this manuscript have no conflict of interest to declare.

REFERENCES

1. Lindahl T. Instability and decay of the primary structure of DNA. Nature. 1993; 362:709-715.

2. Krokan HE et al. Base excision repair of DNA in mammalian cells. FEBS Lett. 2000; 476:73-77.

3. Arczewska KD et al. The contribution of DNA base damage to human cancer is modulated by the base excision repair interaction network. Crit Rev Oncog. 2008; 14:217-273.

4. Barnes DE and Lindahl T. Repair and genetic consequences of endogenous DNA base damage in mammalian cells. Annu Rev Genet. 2004; 38:445-476.

5. Shatilla A and Ramotar D. Embryonic extracts derived from the nematode Caenorhabditis elegans remove uracil from DNA by the sequential action of uracil-DNA glycosylase and AP (apurinic/apyrimidinic) endonuclease. Biochem J. 2002; 365:547-553.

6. Nakamura N et al. Cloning and characterization of uracil-DNA glycosylase and the biological consequences of the loss of its function in the nematode Caenorhabditis elegans. Mutagenesis. 2008; 23:407-413.

7. Morinaga H et al. Purification and characterization of Caenorhabditis elegans NTH, a homolog of human endonuclease III: essential role of N-terminal region. DNA Repair (Amst). 2009; 8:844-851.

8. Olsen A, Vantipalli MC, and Lithgow GJ. Using Caenorhabditis elegans as a model for aging and age-related diseases. Ann N Y Acad Sci. 2006; 1067:120-128.

9. Denver DR et al. The relative roles of three DNA repair pathways in preventing Caenorhabditis elegans mutation accumulation. Genetics. 2006; 174:57-65.

10. Reardon JT et al. In vitro repair of oxidative DNA damage by human nucleotide excision repair system: possible explanation for neurodegeneration in xeroderma pigmentosum patients. Proc Natl Acad Sci U S A. 1997; 94:9463-9468.

11. Swanson R et al. Overlapping specificities of base excision repair, nucleotide excision repair, recombination, and translesion synthesis pathways for DNA base damage in Saccharomyces cerevisiae. Mol Cell Biol. 1999; 19:2929-2935.

12. Boiteux S, Gellon L, and Guibourt N. Repair of 8-oxoguanine in Saccharomyces cerevisiae: interplay of DNA repair and replication mechanisms. Free Radical Biology and Medicine. 2002; 32:1244-1253.

13. Meyer JN et al. Decline of nucleotide excision repair capacity in aging Caenorhabditis elegans. Genome Biol. 2007; 8:R70.

14. Aboussekhra A et al. Mammalian DNA nucleotide excision repair reconstituted with purified protein components. Cell. 1995; 80:859-868.

15. Hartman PS and Herman RK Radiation-sensitive mutants of Caenorhabditis elegans. Genetics. 1982; 102:159-178.

16. Hartman PS et al. Excision repair of UV radiation-induced DNA damage in Caenorhabditis elegans. Genetics. 1989; 122:379-385.

17. Hyun M et al. Longevity and resistance to stress correlate with DNA repair capacity in Caenorhabditis elegans. Nucleic Acids Res. 2008; 36:1380-1389.

18. Kirkwood TB. Understanding the odd science of aging. Cell. 2005; 120:437-447.

19. Garinis GA et al. DNA damage and ageing: new-age ideas for an age-old problem. Nat Cell Biol. 2008; 10:1241-1247.

20. Harman D. Aging: a theory based on free radical and radiation chemistry. J Gerontol. 1956; 11:298-300.

21. van der Pluijm I et al. Impaired genome maintenance suppresses the growth hormone--insulin-like growth factor 1 axis in mice with Cockayne syndrome. PLoS Biol. 2007; 5: e2.

22. Evert BA et al. Spontaneous DNA damage in Saccharomyces cerevisiae elicits phenotypic properties similar to cancer cells. J Biol Chem. 2004; 279:22585-22594.

23. Salmon TB et al. Biological consequences of oxidative stress-induced DNA damage in Saccharomyces cerevisiae. Nucleic Acids Res. 2004; 32:3712-3723.

24. Greiss S et al. Transcriptional profiling in C. elegans suggests DNA damage dependent apoptosis as an ancient function of the p53 family. BMC Genomics. 2008; 9:334.

25. Antebi A. Genetics of aging in Caenorhabditis elegans. PLoS Genet. 2007; 3:1565-1571.

26. Murphy CT et al. Genes that act downstream of DAF-16 to influence the lifespan of Caenorhabditis elegans. Nature. 2003; 424:277-283.

27. McElwee J, Bubb K, and Thomas JH. Transcriptional outputs of the Caenorhabditis elegans forkhead protein DAF-16. Aging Cell. 2003; 2:111-121**.**

28. Johnson TE et al. Longevity genes in the nematode Caenorhabditis elegans also mediate increased resistance to stress and prevent disease. J Inherit Metab Dis. 2002; 25:197-206.

29. Wolf M et al. The MAP kinase JNK-1 of Caenorhabditis elegans: location, activation, and influences over temperature-dependent insulin-like signaling, stress responses, and fitness. J Cell Physiol. 2008; 214:721-729.

30. Honda Y and Honda S. Oxidative stress and life span determination in the nematode Caenorhabditis elegans. Ann N Y Acad Sci. 2002; 959:466-474.

31. Murphy CT, Lee SJ, and Kenyon C. Tissue entrainment by feedback regulation of insulin gene expression in the endoderm of Caenorhabditis elegans. Proc Natl Acad Sci U S A. 2007; 104: 19046-19050.
32. Kahn NW et al. Proteasomal dysfunction activates the transcription factor SKN-1 and produces a selective oxidative-stress response in Caenorhabditis elegans. Biochem J. 2008; 409:205-213.
33. Sheaffer KL, Updike DL, and Mango SE. The Target of Rapamycin pathway antagonizes pha-4/FoxA to control development and aging. Curr Biol. 2008; 18:1355-1364.
34. Salinas LS, Maldonado E, and Navarro RE. Stress-induced germ cell apoptosis by a p53 independent pathway in Caenorhabditis elegans. Cell Death Differ. 2006; 13:2129-2139.
35. Kondo M et al. The p38 signal transduction pathway participates in the oxidative stress-mediated translocation of DAF-16 to Caenorhabditis elegans nuclei. Mech Ageing Dev. 2005; 126:642-647.
36. Lee SJ, Murphy CT, and Kenyon C. Glucose shortens the life span of C. elegans by downregulating DAF-16/FOXO activity and aquaporin gene expression. Cell Metab. 2009; 10: 379-391.
37. Pothof J et al. Identification of genes that protect the C. elegans genome against mutations by genome-wide RNAi. Genes Dev. 2003; 17:443-448.
38. van Haaften G et al. Gene interactions in the DNA damage-response pathway identified by genome-wide RNA-interference analysis of synthetic lethality. Proc Natl Acad Sci U S A. 2004; 101:12992-12996.
39. Trenz K, Errico A, and Costanzo V. Plx1 is required for chromosomal DNA replication under stressful conditions. Embo J. 2008; 27:876-885.
40. Takaki T et al. Polo-like kinase 1 reaches beyond mitosis--cytokinesis, DNA damage response, and development. Curr Opin Cell Biol. 2008; 20:650-660.
41. Mishima M, Kaitna S., and Glotzer M. Central spindle assembly and cytokinesis require a kinesin-like protein/RhoGAP complex with microtubule bundling activity. Dev Cell. 2002; 2:41-54.
42. Woodward AM et al. Excess Mcm2-7 license dormant origins of replication that can be used under conditions of replicative stress. J Cell Biol. 2006; 173:673-683.
43. Astin JW, O'Neil NJ, and Kuwabara PE. Nucleotide excision repair and the degradation of RNA pol II by the Caenorhabditis elegans XPA and Rsp5 orthologues, RAD-3 and WWP-1. DNA Repair (Amst) 2008; 7:267-280.
44. Kenyon C. The plasticity of aging: insights from long-lived mutants. Cell 2005; 120:449-460.
45. Rusyn I et al. Transcriptional networks in S. cerevisiae linked to an accumulation of base excision repair intermediates. PLoS ONE 2007; 2:e1252.
46. Rowe LA, Degtyareva N. and Doetsch PW. DNA damage-induced reactive oxygen species (ROS) stress response in Saccharomyces cerevisiae. Free Radic Biol Med. 2008; 45:1167-1177.
47. Garinis GA et al. Persistent transcription-blocking DNA lesions trigger somatic growth attenuation associated with longevity. Nat Cell Biol. 2009; 11:604-615.
48. Kuraoka I et al. Removal of oxygen free-radical-induced 5',8-purine cyclodeoxynucleosides from DNA by the nucleotide excision-repair pathway in human cells. Proc Natl Acad Sci U S A 2000; 97: 3832-3837.
49. Brenner S. The genetics of Caenorhabditis elegans. Genetics. 1974; 77:71-94.
50. Shannon P et al. Cytoscape: a software environment for integrated models of biomolecular interaction networks. Genome Res. 2003; 13:2498-2504.
51. Maere S, Heymans K. and Kuiper M. BiNGO: a Cytoscape plugin to assess overrepresentation of gene ontology categories in biological networks. Bioinformatics. 2005; 21:3448-3849.
52. Dennis G Jr. et al. DAVID: Database for Annotation, Visualization, and Integrated Discovery. Genome Biol. 2003; 4:P3.
53. Huang da W, Sherman BT, and Lempicki RA. Systematic and integrative analysis of large gene lists using DAVID bioinformatics resources. Nat Protoc. 2009; 4:44-57.
54. Alexeyenko A and Sonnhammer EL. Global networks of functional coupling in eukaryotes from comprehensive data integration. Genome Res. 2009; 19:1107-1116.
55. Przybysz AJ et al. Increased age reduces DAF-16 and SKN-1 signaling and the hormetic response of Caenorhabditis elegans to the xenobiotic juglone. Mech Ageing Dev. 2009; 130: 357-**369.**
56. Kenyon C et al. A C. elegans mutant that lives twice as long as wild type. Nature 1993; 366:461-464.

SUPPLEMENTAL DATA

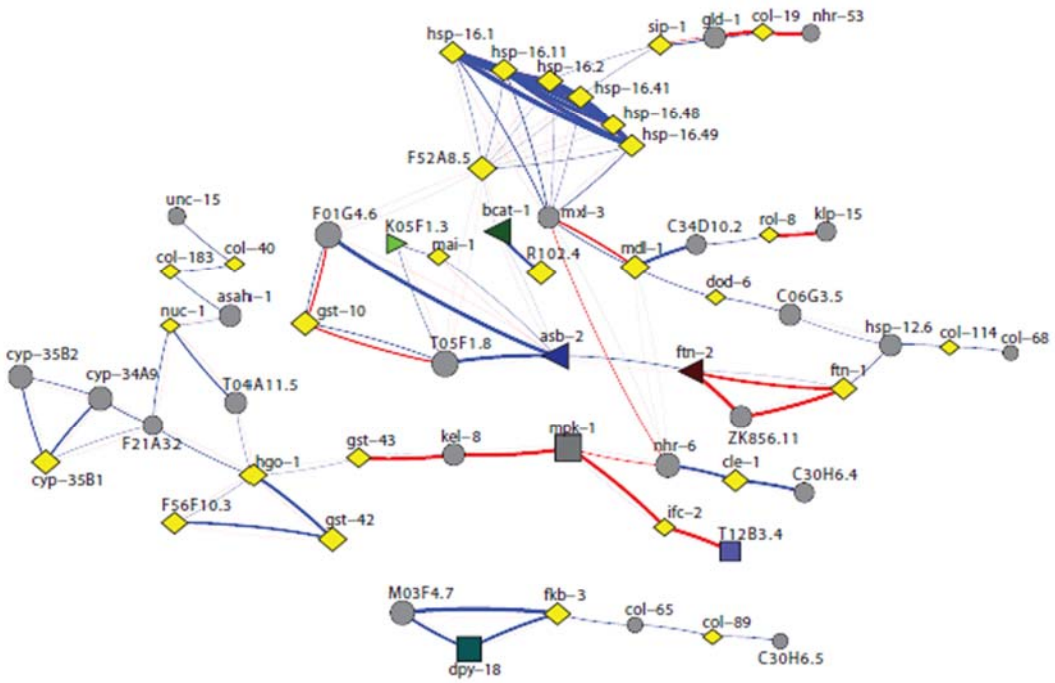

Supplemental Figure 1. Network analysis of downregulated genes within the enriched GO clusters in *xpa-1*

The data of **Supplemental Tables SI, SIII and SIV** are found at link in full text version of this manuscript.

Supplemental Table SII: Overlapping genes in *aqp-1* and *nth-1* and *xpa-1*

Genes	Description	*xpa-1*	*nth-1*	*aqp-1*
ins-7	insulin-like peptide	-8,80	-3,00	1,99
lys-7	an antimicrobial lysozyme	-3,36	-3,40	2,09
hsp-12.6	small heat shock protein	<1,8 (- regulated)	<1,8 (negatively regulated)	2,16
spp-18	SaPosin-like Protein family	-4,06	-2,54	2,38
F46B6.8	triglyceride lipase-cholesterol esterase	-3,34	-3,43	2,43
T24C4.4	unknown	-2,39	<1,8 (similarly regulated)	2,66
mtl-1	copper-binding (detoxifying) metallothionein	-2,42	-2,53	4,41

Genes found to be significantly differentially expressed in an *aqp-1* mutant, as analyzed in [40], were extracted and compared to transcripts in our microarray data set for *nth-1* and *xpa-1*. All 7 transcripts are regulated in a similar direction in the *xpa-1* mutant and 6 out of 7 in the *nth-1* mutant, as AQP-1 is upregulated here and absent in *aqp-1*.

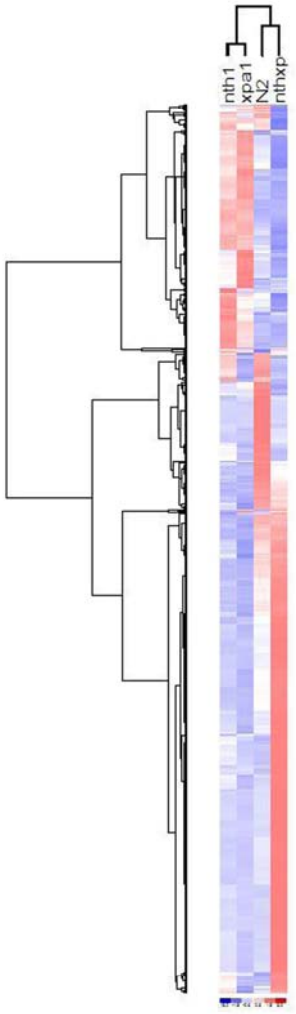

Supplemental Figure 2. Hierarchical clustering between the transcriptomic profiles of N2, *nth-1,/ /xpa-1/, and /nth-1;xpa-1/*

Supplemental Table SV. Gene Ontology classes enriched in BER mutant from Evert et al. 2004

GO ID	Description	p-value	Adjusted p-value
22403	cell cycle phase	6.91E-04	0.097223
22402	cell cycle process	2.08E-03	0.14631
6260	DNA replication	8.30E-05	0.021717
43284	biopolymer biosynthetic process	3.28E-02	0.75578
43283	biopolymer metabolic process	9.25E-05	0.021717
6259	DNA metabolic process	1.33E-02	0.50663
10467	gene expression	3.72E-01	0.89665
7049	cell cycle	8.30E-05	0.021717
6397	mRNA processing	5.79E-05	0.021717
7067	mitosis	1.73E-04	0.03482
6394	RNA processing	6.56E-03	0.35508
6139	nucleobase, nucleoside, nucleotide and nucleic acid metabolic process	8.80E-05	0.021717
87	M phase of mitotic cell cycle	2.29E-04	0.040386
3673	Gene_Ontology	1	1
16071	mRNA metabolic process	1.07E-03	0.10414
16070	RNA metabolic process	7.91E-04	0.10131
44237	cellular metabolic process	1.43E-01	0.75578
44238	primary metabolic process	1.37E-01	0.75578
9058	biosynthetic process	9.93E-01	1
9059	macromolecule biosynthetic process	8.57E-01	1
278	mitotic cell cycle	4.72E-05	0.021717
279	M phase	2.36E-03	0.15796
8150	biological_process	1	1
8151	cellular process	1.17E-03	0.10414
43170	macromolecule metabolic process	7.05E-03	0.36527
8152	metabolic process	2.07E-01	0.8488

Supplemental Table SV. Gene Ontology classes enriched in NER mutant from Evert et al. 2004

GO ID	Description	p-value	Adjusted p-value
50791	regulation of biological process	3.25E-08	3.5252E-06
9451	RNA modification	2.47E-04	0.0077878
43285	biopolymer catabolic process	1.56E-04	0.0054788
43284	biopolymer biosynthetic process	3.53E-02	0.31648
43283	biopolymer metabolic process	1.67E-20	3.6264E-17
43632	modification-dependent macromolecule catabolic process	1.82E-06	0.00011961
6350	transcription	1.06E-09	1.7701E-07
6357	regulation of transcription from RNA polymerase II promoter	3.14E-04	0.0094851
51179	localization	1.96E-02	0.21161
6355	regulation of transcription, DNA-dependent	5.34E-11	1.2893E-08
7067	mitosis	5.15E-08	4.4777E-06
43412	biopolymer modification	1.26E-16	9.0907E-14
19219	regulation of nucleobase, nucleoside, nucleotide and nucleic acid metabolic process	2.72E-11	7.3969E-09
16071	mRNA metabolic process	1.61E-06	0.0001093
16070	RNA metabolic process	6.35E-19	6.8996E-16
16072	rRNA metabolic process	1.27E-05	0.00062762
51234	establishment of localization	2.36E-02	0.23851
9058	biosynthetic process	9.81E-01	1
9059	macromolecule biosynthetic process	9.04E-01	1
9056	catabolic process	1.34E-02	0.16486
9057	macromolecule catabolic process	8.11E-03	0.11986
278	mitotic cell cycle	1.08E-08	1.5586E-06
279	M phase	3.11E-04	0.0094851
22403	cell cycle phase	2.29E-05	0.001035
22402	cell cycle process	2.74E-05	0.0011908
6468	protein amino acid phosphorylation	2.61E-05	0.0011555
40023	establishment of nucleus localization	2.39E-04	0.0076369
8104	protein localization	3.98E-06	0.00024027
19538	protein metabolic process	6.19E-01	0.98988
6374	nuclear mRNA splicing, via spliceosome	2.66E-08	3.0412E-06
48523	negative regulation of cellular process	1.53E-03	0.033849
16568	chromatin modification	1.50E-05	0.00072322
7049	cell cycle	3.86E-05	0.0015513
43161	proteasomal ubiquitin-dependent protein catabolic process	5.78E-05	0.0021643

19222	regulation of metabolic process	1.45E-04	0.0051619
819	sister chromatid segregation	3.49E-08	3.6073E-06
15031	protein transport	1.56E-05	0.00073851
9890	negative regulation of biosynthetic process	3.22E-04	0.0095787
6810	Transport	4.80E-02	0.38345
46907	intracellular transport	2.21E-05	0.0010194
16359	mitotic sister chromatid segregation	4.73E-08	4.2837E-06
9892	negative regulation of metabolic process	2.79E-04	0.0086566
51603	proteolysis involved in cellular protein catabolic process	9.68E-06	0.00048888
10498	proteasomal protein catabolic process	5.78E-05	0.0021643
45449	regulation of transcription	2.35E-11	7.3011E-09
9889	regulation of biosynthetic process	6.95E-04	0.018879
7059	chromosome segregation	5.44E-06	0.00031909
30163	protein catabolic process	1.01E-04	0.003654
60255	regulation of macromolecule metabolic process	9.88E-04	0.024955
48519	negative regulation of biological process	1.04E-03	0.025837
43170	macromolecule metabolic process	6.27E-10	1.1353E-07
33036	macromolecule localization	2.45E-06	0.00015653
16043	cellular component organization and biogenesis	2.83E-05	0.0012045
31323	regulation of cellular metabolic process	6.92E-04	0.018879
31324	negative regulation of cellular metabolic process	2.17E-04	0.0071475
6464	protein modification process	3.57E-13	1.5516E-10
44248	cellular catabolic process	5.35E-02	0.41819
6397	mRNA processing	1.28E-07	0.000010295
6394	RNA processing	1.62E-07	0.00001259
6395	RNA splicing	1.07E-07	8.9535E-06
87	M phase of mitotic cell cycle	2.38E-08	0.000002873
6399	tRNA metabolic process	2.96E-05	0.0012114
6508	proteolysis	5.78E-02	0.43859
44237	cellular metabolic process	2.93E-05	0.0012114
44238	primary metabolic process	2.12E-07	0.000015873
6511	ubiquitin-dependent protein catabolic process	8.63E-06	0.00045728
375	RNA splicing, via transesterification reactions	2.15E-08	2.7473E-06
377	RNA splicing, via transesterification reactions with bulged adenosine as nucleophile	1.63E-08	2.2143E-06

65007	biological regulation	4.04E-08	3.9905E-06
8150	biological_process	1	1
74	regulation of cell cycle	5.50E-05	0.0021333
8151	cellular process	5.90E-09	9.1482E-07
8152	metabolic process	4.65E-05	0.0018374
7001	chromosome organization and biogenesis	3.32E-07	0.000023249
6796	phosphate metabolic process	2.10E-03	0.043887
6793	phosphorus metabolic process	1.49E-02	0.18021
44265	cellular macromolecule catabolic process	1.52E-02	0.18091
51656	establishment of organelle localization	9.29E-02	0.56062
44267	cellular protein metabolic process	6.22E-01	0.98988
51252	regulation of RNA metabolic process	1.40E-10	3.0468E-08
6338	chromatin remodeling	1.59E-04	0.0054797
44260	cellular macromolecule metabolic process	6.37E-01	0.98988
10467	gene expression	1.75E-02	0.19845
10468	regulation of gene expression	1.98E-03	0.042124
6139	nucleobase, nucleoside, nucleotide and nucleic acid metabolic process	1.92E-14	1.0422E-11
51640	organelle localization	2.52E-01	0.85288
51641	cellular localization	3.38E-06	0.00020981
3673	Gene_Ontology	1	1
45184	establishment of protein localization	6.95E-06	0.00039717
51649	establishment of localization in cell	7.19E-06	0.00040046
44257	cellular protein catabolic process	1.86E-04	0.0063051
7154	cell communication	9.31E-06	0.00048166
51647	nucleus localization	2.39E-04	0.0076369
6996	organelle organization and biogenesis	2.54E-10	5.0099E-08
6325	establishment and/or maintenance of chromatin architecture	3.76E-04	0.010757
16197	endosome transport	6.53E-05	0.0024029
51244	regulation of cellular process	3.31E-07	0.000023249
10556	regulation of macromolecule biosynthetic process	1.17E-03	0.027818
6914	autophagy	4.23E-08	0.000003997
16310	phosphorylation	3.84E-03	0.069565
16192	vesicle-mediated transport	1.93E-04	0.0064581
43687	post-translational protein modification	2.03E-12	7.3582E-10
19941	modification-dependent protein catabolic process	8.63E-06	0.00045728

Supplemental Table SV. Gene Ontology classes enriched in BERNER mutant from Evert et al. 2004

BERNER	Description	p-value	Adjusted p-value
16043	cellular component organization and biogenesis	1.15E-04	0.0048336
31323	regulation of cellular metabolic process	1.89E-06	0.00015066
31324	negative regulation of cellular metabolic process	1.71E-04	0.0061898
50791	regulation of biological process	2.70E-09	5.8504E-07
6464	protein modification process	1.59E-02	0.15882
6323	DNA packaging	2.50E-04	0.0084307
31325	positive regulation of cellular metabolic process	1.03E-03	0.022008
44248	cellular catabolic process	7.48E-01	0.95503
43285	biopolymer catabolic process	7.00E-02	0.4042
43284	biopolymer biosynthetic process	3.64E-03	0.052678
43283	biopolymer metabolic process	8.49E-07	0.000075776
6350	transcription	2.24E-06	0.00016156
6259	DNA metabolic process	1.43E-03	0.028105
6355	regulation of transcription, DNA-dependent	2.86E-10	1.0866E-07
7067	mitosis	4.34E-06	0.00026332
87	M phase of mitotic cell cycle	2.68E-06	0.00018526
6399	tRNA metabolic process	1.22E-02	0.13789
43412	biopolymer modification	2.38E-03	0.039645
19219	regulation of nucleobase, nucleoside, nucleotide and nucleic acid metabolic process	6.02E-11	6.3277E-08
16070	RNA metabolic process	7.94E-08	8.6131E-06
51869	response to stimulus	5.80E-02	0.37839
44237	cellular metabolic process	1.34E-01	0.54932
16078	tRNA catabolic process	1.05E-04	0.0046846
44238	primary metabolic process	5.92E-02	0.37839
45935	positive regulation of nucleobase, nucleoside, nucleotide and nucleic acid metabolic process	1.14E-03	0.023988
9058	biosynthetic process	7.47E-01	0.95503

9059	macromolecule biosynthetic process	2.30E-01	0.65903
9056	catabolic process	6.91E-01	0.94702
6974	response to DNA damage stimulus	1.64E-07	0.000016609
9057	macromolecule catabolic process	2.67E-01	0.67632
45934	negative regulation of nucleobase, nucleoside, nucleotide and nucleic acid metabolic process	1.15E-04	0.0048336
278	mitotic cell cycle	4.13E-09	6.2634E-07
279	M phase	9.72E-06	0.00052306
65007	biological regulation	6.75E-08	7.8862E-06
8150	biological_process	1	1
8151	cellular process	1.24E-03	0.025781
74	regulation of cell cycle	1.32E-04	0.0054266
75	cell cycle checkpoint	1.40E-04	0.0055301
8152	metabolic process	2.10E-01	0.61785
22403	cell cycle phase	5.46E-08	0.000006906
22402	cell cycle process	4.29E-10	1.3031E-07
7001	chromosome organization and biogenesis	2.99E-06	0.00019715
6401	RNA catabolic process	3.49E-01	0.75539
6950	response to stress	8.51E-02	0.4583
6281	DNA repair	9.99E-06	0.00052306
44265	cellular macromolecule catabolic process	4.24E-01	0.82681
44267	cellular protein metabolic process	9.90E-01	1
51252	regulation of RNA metabolic process	8.34E-11	6.3277E-08
6338	chromatin remodeling	1.74E-06	0.00014642
44260	cellular macromolecule metabolic process	9.93E-01	1
19538	protein metabolic process	9.83E-01	1
48523	negative regulation of cellular process	1.61E-04	0.0061024
51254	positive regulation of RNA metabolic process	2.20E-04	0.007603
16568	chromatin modification	2.72E-05	0.0013303

10467	gene expression	1.53E-02	0.15479
10468	regulation of gene expression	6.59E-06	0.00038484
7049	cell cycle	2.24E-10	1.0866E-07
19222	regulation of metabolic process	2.20E-06	0.00016156
6139	nucleobase, nucleoside, nucleotide and nucleic acid metabolic process	3.69E-09	6.2316E-07
16458	gene silencing	4.57E-05	0.002168
9890	negative regulation of biosynthetic process	3.09E-04	0.0099772
3673	Gene_Ontology	1	1
6996	organelle organization and biogenesis	2.83E-07	0.00002689
9893	positive regulation of metabolic process	1.03E-03	0.022008
9892	negative regulation of metabolic process	1.93E-04	0.006816
6325	establishment and/or maintenance of chromatin architecture	1.70E-04	0.0061898
45449	regulation of transcription	7.75E-10	1.9606E-07
51242	positive regulation of cellular process	8.07E-04	0.018294
9889	regulation of biosynthetic process	3.59E-06	0.00022728
10556	regulation of macromolecule biosynthetic process	7.76E-06	0.00043635
51244	regulation of cellular process	3.38E-09	6.2316E-07
7059	chromosome segregation	9.66E-05	0.0044448
6914	autophagy	1.24E-08	1.7147E-06
60255	regulation of macromolecule metabolic process	1.26E-05	0.00063573
48519	negative regulation of biological process	1.42E-04	0.0055301
48518	positive regulation of biological process	9.27E-04	0.020391
43687	post-translational protein modification	2.99E-04	0.0098537
43170	macromolecule metabolic process	5.05E-04	0.013809

Supplemental Table SV. Gene Ontology enriched classes unique to each mutant from Evert et al. 2004

BERNER	BERNER GO	BER	BER GO	NER	NER GO
		6260	DNA replication	375	RNA splicing, via transesterification reactions
6281	DNA repair			377	RNA splicing, via transesterification reactions with bulged adenosine as nucleophile
				9451	RNA modification
51869	response to stimulus			6357	regulation of transcription from RNA polymerase II promoter
75	cell cycle checkpoint			6374	nuclear mRNA splicing, via spliceosome
6950	response to stress			6395	RNA splicing
6974	response to DNA damage stimulus			16072	rRNA metabolic process
6323	DNA packaging			6468	protein amino acid phosphorylation
16458	gene silencing			16310	phosphorylation
				6793	phosphorus metabolic process
45934	negative regulation of nucleobase, nucleoside, nucleotide and nucleic acid metabolic process			6796	phosphate metabolic process
45935	positive regulation of nucleobase, nucleoside, nucleotide and nucleic acid metabolic process				
				7154	cell communication
48518	positive regulation of biological process				
51242	positive regulation of cellular process			6508	proteolysis
9893	positive regulation of metabolic process			6511	ubiquitin-dependent protein catabolic process
31325	positive regulation of cellular metabolic process			51603	proteolysis involved in cellular protein catabolic process
				10498	proteasomal protein catabolic process
16078	tRNA catabolic process			19941	modification-dependent protein catabolic process
6401	RNA catabolic process			30163	protein catabolic process
51254	positive regulation of RNA metabolic process			43161	proteasomal ubiquitin-dependent protein catabolic process
				43632	modification-dependent macromolecule catabolic process
65007	biological regulation			44257	cellular protein catabolic process
				6810	transport
				8104	protein localization
				15031	protein transport
				16192	vesicle-mediated transport
				16197	endosome transport
				46907	intracellular transport
				45184	establishment of protein localization

45184	establishment of protein localization
51179	localization
51234	establishment of localization
51640	organelle localization
51641	cellular localization
51647	nucleus localization
51649	establishment of localization in cell
51656	establishment of organelle localization
33036	macromolecule localization
40023	establishment of nucleus localization
16359	mitotic sister chromatid segregation
819	sister chromatid segregation